JOURNAL OF SYNCHROTRON RADIATION
ISSN 1600-5775

Flattening filter for Gaussian-shaped monochromatic X-ray beams: an application to breast computed tomography

Sandro Donato,[a,b] Fulvia Arfelli,[a,b] Luca Brombal,[a,b]* Renata Longo,[a,b] Andrea Pinto,[c] Luigi Rigon[a,b] and Diego Dreossi[d]

[a]Department of Physics, University of Trieste, 34127 Trieste, Italy, [b]INFN Division of Trieste, 34127 Trieste, Italy, [c]Department of Medicine, Surgery and Health Sciences, University of Trieste, 34127 Trieste, Italy, and [d]Elettra-Sincrotrone Trieste SCpA, 34149 Trieste, Italy. *Correspondence e-mail: luca.brombal@ts.infn.it

Received 24 July 2019
Accepted 11 December 2019

Edited by P. A. Pianetta, SLAC National Accelerator Laboratory, USA

Keywords: beam filtering; breast computed tomography; Gaussian beam.

The vertical intensity distribution of synchrotron-based X-ray beams usually has a Gaussian profile encompassing large intensity variations. For biomedical imaging applications this may entail sub-optimal dose distributions and large fluctuations in terms of image noise. Commonly, planar metallic filters coupled with absorbing slits systems are applied to adjust the delivered flux and to limit intensity variations, respectively. The latter results in a reduction of the effective beam size. A flattening filter that counterbalances the transverse inhomogeneity, while retaining a sufficient flux, has been developed in the context of a monochromatic phase-contrast breast computed tomography application, ongoing at the Elettra synchrotron facility. The implementation of the new filtration system results in homogeneous intensity (hence dose) distribution and signal-to-noise ratio across the imaged volume. Finally, and most importantly, it allows a wider portion of the beam to be used, directly translating into a major (∼40%) reduction of the overall scan time for samples requiring a field of view larger than the beam size (*i.e.* multiple translation steps).

1. Introduction

Besides the high coherence, X-rays produced by synchrotrons are, in general, several orders of magnitude more intense with respect to conventional sources. For this reason, many biomedical imaging applications require beam filtration to deliver acceptable dose levels within a given exposure time (Bravin *et al.*, 2013; Rigon, 2014). This is usually performed by inserting metallic sheets or slabs that reduce the overall beam intensity without affecting its spatial distribution (or 'shape'). When considering synchrotron radiation produced by bending magnets, the beam vertical (*i.e.* orthogonal to the electrons orbit plane) intensity distribution is well described by a Gaussian function (Wiedemann, 2003), that leads to an undesired non-uniform dose distribution on the sample in the vertical direction. In terms of image quality this means that, especially for tomographic applications, the signal-to-noise-ratio (SNR) decreases from the central maximum towards the tails. To limit such non-uniformity, in most cases only the central part of the beam is used for imaging purposes, while the tails are cut out by absorbing (*e.g.* tungsten) slits. Despite being easy to implement, this approach is not optimal for applications requiring tomographic scans of large samples since the reduction of the beam vertical dimension means an increase in the number of vertical scans required to image the whole volume and, as a consequence, an increase in the overall scan duration.

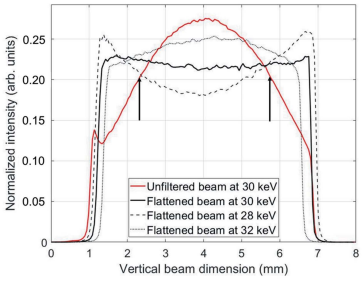

To overcome the non-uniformity while using the full beam vertical dimension, an *ad hoc* parabolic-shaped flattening filter has been designed for monochromatic beam applications and implemented at the SYRMEP beamline of the Elettra synchrotron facility (Trieste, Italy). The filtration system has been developed in the context of the SYRMA-3D project, aiming at setting up a phase-contrast synchrotron radiation (SR) breast computed tomography (BCT) clinical study (Longo *et al.*, 2016, 2019). Up to now, a slit system (Densimet® tungsten alloy), coupled with planar aluminium filters, has been routinely used. The system defines a vertical beam dimension of 3.5 mm at the sample position encompassing intensity variations of about 30% (from center to edge) at energies around 30 keV. Conversely, the net effect of the developed filter is to produce a nearly constant vertical intensity distribution, allowing both to uniformly deliver the radiation dose, hence producing images with a uniform SNR, and to use a wider vertical portion of the beam (more than 5 mm), hence reducing the number of scans required for large samples. The usefulness of the new filtration system is also demonstrated on tomographic images of surgical breast specimens acquired with low delivered dose following the clinically oriented procedure described by Longo *et al.* (2019).

2. Materials and methods

2.1. Filter design

To obtain a flat transmitted intensity distribution we are looking for a filter, described by the function $F(y;E)$, that satisfies the following equation,

$$I_{\rm f}(y;E) = I(y;E)\exp\left[-\mu_{\rm f}(E)\,F(y;E)\right] = k, \qquad (1)$$

where $I(y;E)$ is the energy-dependent (E) incoming beam intensity distribution along the vertical direction (y), $\mu_{\rm f}(E)$ is the attenuation coefficient of the filter and $I_{\rm f}(y;E)$ is the flattened transmitted beam, whose constant intensity is equal to a transmitted fraction k of the maximum of the input beam. By assuming that the unfiltered beam has a Gaussian vertical spatial distribution, $I(y;E) \propto \exp\{-[y/2\sigma_y(E)]^2\}$, with an energy-dependent standard deviation $\sigma_y(E)$, the filter shape can be computed by solving equation (1), and it reads

$$F(y;E) = -\frac{y^2}{2\sigma_y^2(E)\,\mu_{\rm f}(E)} - \frac{\ln k}{\mu_{\rm f}(E)}. \qquad (2)$$

Therefore, the desired filter has a parabolic shape whose depth ($d_{\rm f}$, *i.e.* size along the beam propagation direction) and height ($h_{\rm f}$, *i.e.* size along the vertical dimension of the beam) are, respectively,

$$d_{\rm f} = \frac{|\ln k|}{\mu_{\rm f}(E)}, \qquad h_{\rm f} = 2\sigma_y(E)\left(2|\ln k|\right)^{1/2}. \qquad (3)$$

At this point it can be noted that filter depth depends both on the filter material, through its attenuation coefficient, and on the desired intensity fraction of the impinging beam. Conversely, filter height is dependent on the beam vertical dimension and its intensity fraction while it is independent of the filter material.

2.2. Filter implementation and image acquisition

An aluminium filter has been designed for an energy of 30 keV, that lies within the optimal range for SR BCT (Baran *et al.*, 2017; Longo *et al.*, 2019). At this energy the beam standard deviation at sample position, *i.e.* 30 m from the X-ray source, is σ_y(30 keV) = 1.8 mm. Since the filter is positioned 4.0 m upstream with respect to the sample, a standard deviation of 1.6 mm has been considered to compensate for the beam magnification. The transmission factor is chosen to be k = 18%, providing sufficient flux for delivering (mean glandular) dose rates up to 0.5 mGy s^{-1} to large (∼10 cm) breast samples. Considering the standard scan time (40 s) for SR BCT examination, as reported in previous studies (Brombal *et al.*, 2019; Longo *et al.*, 2019), this results in doses up to 20 mGy, which corresponds to the 'high-image quality' (*ex vivo*) modality of the SYRMA-3D protocol (Piai *et al.*, 2019). Therefore, in order to match the clinical target dose level of 5 mGy for *in vivo* applications, extra filtration by means of aluminium sheets is needed.

As a general remark, the energy dependence of the filter shape can be seen as a practical drawback of this approach since, in principle, each energy would require an *ad hoc* designed filter. Anyway, as will be clear in the next section, for energies around 30 keV, the manufactured filter is proven to be sufficiently flexible to yield a beam that is more homogeneous with respect to the standard planar filtration system in a range of energies of some keV. If the same filtration approach has to be adapted for lower energies while retaining sufficient flexibility, lighter materials, whose attenuation coefficient is Compton dominated, should be used. As an example, plastic filters (*i.e.* $6 < Z_{\rm eff} < 7$) could be used down to about 20 keV.

Starting from the aforementioned k and σ parameters, the filter has been modeled by a computer-aided design (CAD) software and manufactured with a computer numerical control machine (see Fig. 1). The images are acquired with a large-area CdTe photon-counting detector (Bellazzini *et al.*, 2013; Brombal *et al.*, 2018) featuring a pixel pitch of 60 µm, positioned 1.6 m downstream of the sample (Longo *et al.*, 2019).

3. Results

The flattening filter has been tested at three different energies of 28, 30 and 32 keV. As shown in Fig. 2, when used at the design energy of 30 keV [see panels (*b*) and (*e*)], the filter ensures a beam profile with intensity fluctuations up to 5% and a height of 5.5 mm, whereas the unfiltered beam [panel (*a*)] has, in the same spatial range, a maximum intensity variation of more than 60% around the mean value. Moreover, even considering a smaller portion of the beam (3.5 mm), that would have been selected by using the slit system [black arrows in panel (*e*)], the intensity variation in the unfiltered beam is around 30%. When employed at a beam

energy of 28 keV [panel (*c*)], the filter introduces an excessive attenuation in the central portion of the beam, yielding a cup-shaped profile. Anyway, the observed intensity variation over the entire beam height (5.7 mm) is of the order of 30%, which is half of the variation of the unfiltered beam in the same spatial range. The opposite behavior is found for the 32 keV irradiation [panel (*d*)]: in this case the maximum intensity fluctuation over the whole beam height (5 mm) is of the order of 15%, about four times smaller if compared with the unfiltered beam.

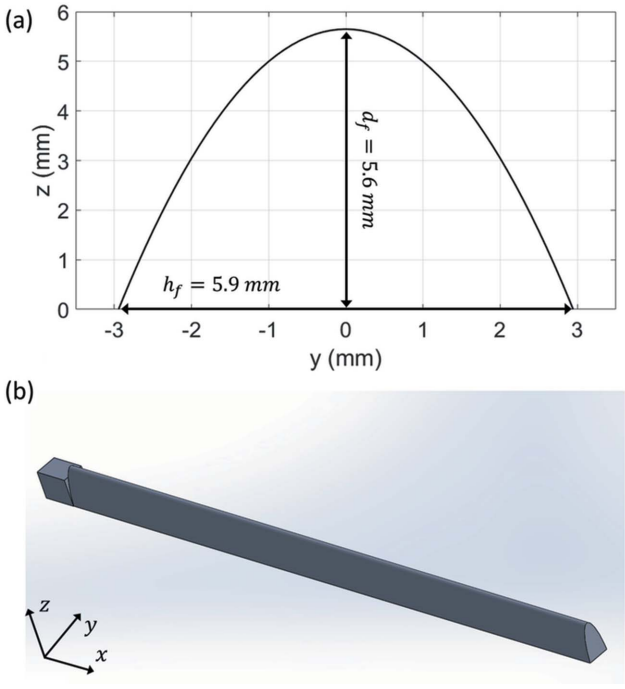

Figure 1
(*a*) Filter parabolic profile optimized for a 30 keV beam and 26 m from the source at SYRMEP beamline and (*b*) its CAD-design.

To demonstrate the effectiveness of the filter in a realistic scenario, the tomographic reconstructions of two mastectomy samples, with similar sizes and compositions, imaged with and without using the flattening filter, have been compared. The scan energy was 32 keV (that is not the optimal energy for the described filter) and the mean glandular dose of 5 mGy was delivered to both samples (Mettivier *et al.*, 2016). The results are summarized in Fig. 3. In panels (*a*) and (*b*), reconstructed details of the sample acquired with no flattening filter are reported considering slices corresponding to the central and the tail regions of the beam, respectively. In the same way, panels (*c*) and (*d*) show slices of the sample acquired with the flattening filter at the center and at the edge positions of the beam. For each slice of both samples, SNR, defined as the ratio between the mean and the standard deviation of gray values within a selected region of interest, is measured on a glandular detail and reported as a function of the slice position in panel (*e*). From the plot it is clear that by using the flattening filter the SNR has a smoother dependence on the slice position with respect to the conventional planar filtration system. Of note, since the radiation dose is more evenly distributed when the filter is used, the measured SNR is lower in the center and higher at the edges of the beam with respect to the beam filtered by using planar filters. Moreover, having a wider portion of the beam useful for imaging purposes [from slightly more than 3 mm to 5 mm for the case reported in Fig. 3(*e*)] translates into a reduction of the scan time for imaging the whole volume of approximately 40%.

4. Discussion and conclusions

Many biomedical imaging applications at synchrotron facilities make use of planar beam filtration systems, resulting in a sub-optimal dose/intensity distribution due to the inherent Gaussian vertical spatial distribution of the produced X-rays. In this communication we demonstrated that this issue can be tackled by using a specifically designed parabolic filter, enabling the shape of the incoming beam to be flattened resulting in intensity fluctuations of a few percent. The latter additionally allows the full height of the beam to be used, thus increasing the illuminated area/volume of the sample acquired in each scan. In view of the *in vivo* phase-contrast BCT application, this improvement is of major importance for three main reasons. Firstly, a homogeneous beam intensity allows the radiation dose to be evenly distributed. Secondly, a flat beam profile results in a constant image noise or SNR across the whole reconstructed volume, thus

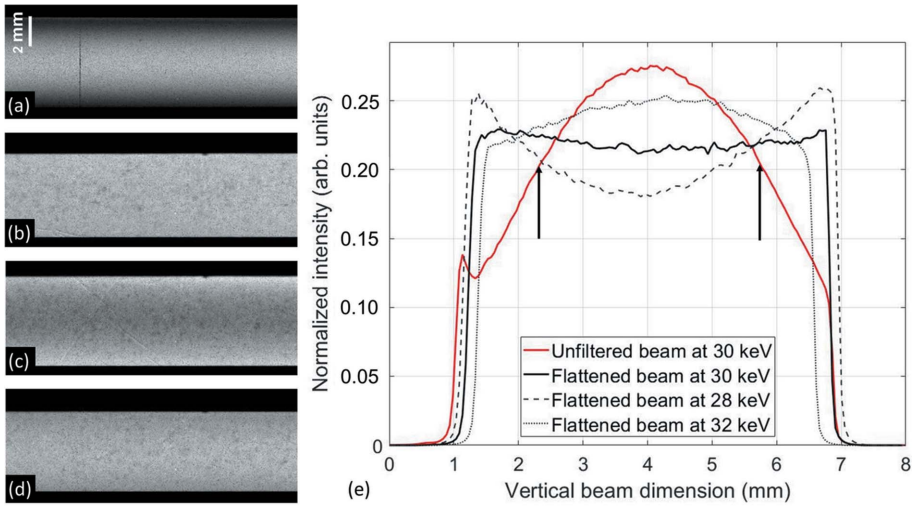

Figure 2
Images of the beam with no filtration (*a*) and flattening filter at 30 keV (*b*), 28 keV (*c*) and 32 keV (*d*). Vertical profiles (*e*) of the beams reported in panels (*a*)–(*d*). Black arrows indicate the position corresponding to the tungsten slits system used for the clinically oriented imaging experiments so far. Profiles in (*e*) are normalized to their area.

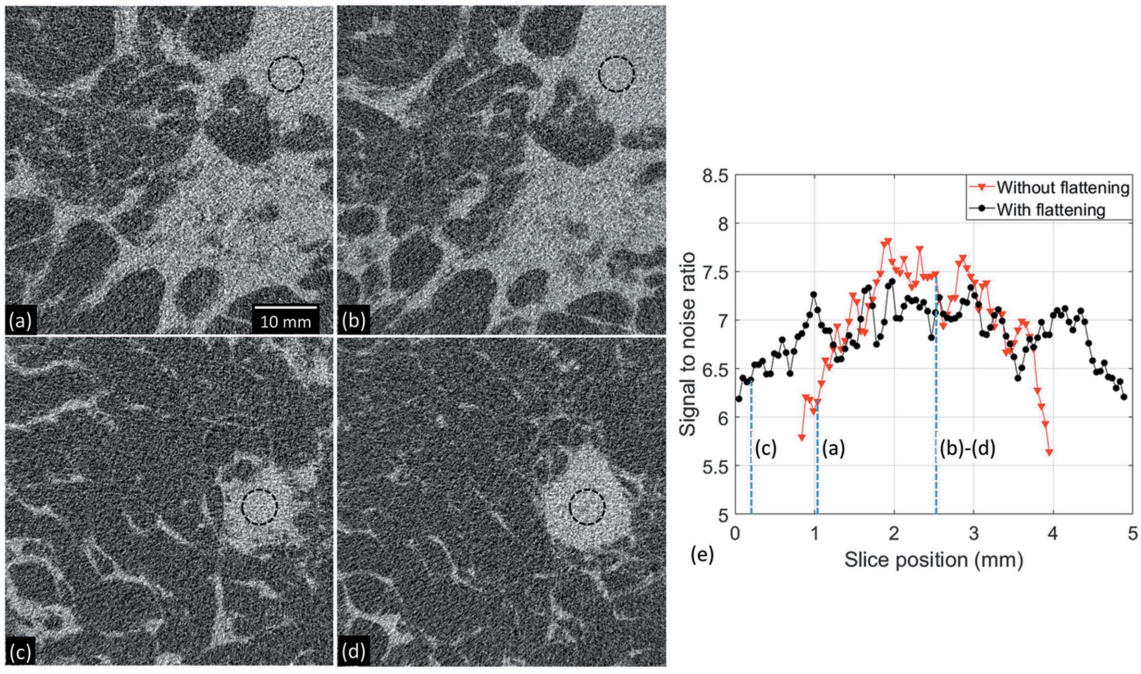

Figure 3
Details of reconstructed slices corresponding to the central portion and to the edge of the vertical field-of-view obtained with a conventional planar filtration system [(*a*) edge, (*b*) center] and with the flattening filter [(*c*) edge, (*d*) center], respectively. (*e*) Plot of SNR as a function of slice position measured within the dashed circles in (*a*)–(*d*) for both filtering configurations. Light-blue dashed lines represent slice positions of panels (*a*)–(*d*).

potentially improving the radiological evaluation. Lastly, the increase of the useful beam height directly translates into a 40% reduction of the overall scan time for imaging the whole breast. This will limit the patient discomfort, hence possible motion artifacts associated with voluntary movement, and it will improve the examination throughput. Finally, the filter proved to be sufficiently flexible in a 4 keV range (centered on the nominal energy of 30 keV), which is of interest for BCT applications.

Acknowledgements

The SYRMA-3D project is supported by Istituto Nazionale di Fisica Nucleare (National Scientific Committee 5 for Technological and Inter-disciplinary Research) and Elettra-Sincrotrone Trieste SCpA. SD is partially supported by Consorzio per la Fisica Trieste.

References

Baran, P., Pacile, S., Nesterets, Y., Mayo, S., Dullin, C., Dreossi, D., Arfelli, F., Thompson, D., Lockie, D., McCormack, M., Taba, S. T., Brun, F., Pinamonti, M., Nickson, C., Hall, C., Dimmock, M., Zanconati, F., Cholewa, M., Quiney, H., Brennan, P. C., Tromba, G. & Gureyev, T. E. (2017). *Phys. Med. Biol.* **62**, 2315–2332.

Bellazzini, R., Spandre, G., Brez, A., Minuti, M., Pinchera, M. & Mozzo, P. (2013). *J. Instrum.* **8**, C02028.

Bravin, A., Coan, P. & Suortti, P. (2013). *Phys. Med. Biol.* **58**, R1–R35.

Brombal, L., Donato, S., Brun, F., Delogu, P., Fanti, V., Oliva, P., Rigon, L., Di Trapani, V., Longo, R. & Golosio, B. (2018). *J. Synchrotron Rad.* **25**, 1068–1077.

Brombal, L., Golosio, B., Arfelli, F., Bonazza, D., Contillo, A., Delogu, P., Donato, S., Mettivier, G., Oliva, P., Rigon, L., Taibi, A., Tromba, G., Zanconati, F. & Longo, R. (2019). *J. Med. Imaging*, **6**, 031402.

Longo, R., Arfelli, F., Bellazzini, R., Bottigli, U., Brez, A., Brun, F., Brunetti, A., Delogu, P., Di Lillo, F., Dreossi, D., Fanti, V., Fedon, C., Golosio, B., Lanconelli, N., Mettivier, G., Minuti, M., Oliva, P., Pinchera, M., Rigon, L., Russo, P., Sarno, A., Spandre, G., Tromba, G. & Zanconati, F. (2016). *Phys. Med. Biol.* **61**, 1634–1649.

Longo, R., Arfelli, F., Bonazza, D., Bottigli, U., Brombal, L., Contillo, A., Cova, M. A., Delogu, P., Di Lillo, F., Di Trapani, V., Donato, S., Dreossi, D., Fanti, V., Fedon, C., Golosio, B., Mettivier, G., Oliva, P., Pacilè, S., Sarno, A., Rigon, L., Russo, P., Taibi, A., Tonutti, M., Zanconati, F. & Tromba, G. (2019). *J. Synchrotron Rad.* **26**, 1343–1353.

Mettivier, G., Fedon, C., Di Lillo, F., Longo, R., Sarno, A., Tromba, G. & Russo, P. (2016). *Phys. Med. Biol.* **61**, 569–587.

Piai, A., Contillo, A., Arfelli, F., Bonazza, D., Brombal, L., Assunta Cova, M., Delogu, P., Di Trapani, V., Donato, S., Golosio, B., Mettivier, G., Oliva, P., Rigon, L., Taibi, A., Tonutti, M., Tromba, G., Zanconati, F. & Longo, R. (2019). *Phys. Med. Biol.* **64**, 155011.

Rigon, L. (2014). *X-ray Imaging with Coherent Sources*, Vol. 4 of *Comprehensive Biomedical Physics.* Elsevier.

Wiedemann, H. (2003). *Particle Accelerator Physics*, pp. 647–686. Berlin: Springer.